The Open University of Sri Lanka
Department of Electrical and Computer Engineering
ECX 6242 – Modern Control Systems
Final Examination – 2011/2012

Date: 2012-03-11 Time: 0930-1230

Answer five questions by selecting at least two questions from each of the sections A and B.

Section A

Q1. A system is represented by the differential equation

$$\frac{d^2y}{dt^2} + 2\frac{dy}{dt} + y = \frac{du}{dt} + u$$

Where $y = output$ and $u = input$.

(a) Describe what are the advantages of state space modelling?

(b) Define the state as $x_1 = y$ and $x_2 = \frac{dy}{dt} - u$ and determine whether the system is controllable.

Q2. Consider the system represented in state variable form

$$\dot{x} = \boldsymbol{A}x + \boldsymbol{B}u$$
$$y = \boldsymbol{C}x + \boldsymbol{D}u$$

where

$$\boldsymbol{A} = \begin{bmatrix} 1 & 1 \\ -5 & -10 \end{bmatrix}, \boldsymbol{B} = \begin{bmatrix} -4 \\ 1 \end{bmatrix}, \boldsymbol{C} = [6 \quad -4] \text{ and } \boldsymbol{D} = [0].$$

(a) Verify that the system is observable and controllable.

(b) If so, design a full-state feedback law and an observer by placing the closed-loop system poles at $s_{1,2} = -1 \pm j$ and the observer poles at $s_{1,2} = -10$.

Q3.

(a) Briefly describe Lyapunov's direct method for the determination of the stability of non-linear systems.

(b) Consider the scalar system

$$\dot{x} = ax^3$$

(i) Show that Lyapunov's linearization method fails to determine the stability of the origin.

(ii) Use Lyapunov's function $V(x) = x^4$ to show that the system is stable for $a < 0$ and unstable for $a > 0$.

(iii) What can you say about the system stability for $a = 0$?

Q4. Consider the system described in state variable form

$$\dot{\boldsymbol{x}}(t) = \boldsymbol{A}\boldsymbol{x}(t) + \boldsymbol{B}u(t)$$

$$y = \boldsymbol{C}\boldsymbol{x}(t)$$

where $\boldsymbol{A} = \begin{bmatrix} 1 & 1 \\ -k_1 & -k_2 \end{bmatrix}$, $\boldsymbol{B} = \begin{bmatrix} 0 \\ 1 \end{bmatrix}$ and $\boldsymbol{C} = [1 \quad -1]$, and where $k_1 \neq k_2$ and both k_1 and k_2 are real numbers.

(a) Compute the state transition matrix $\Phi(t, 0)$.
(b) Compute the eigenvalues of the system matrix $\boldsymbol{A}$.
(c) Compute the roots of the characteristics polynomial.
(d) Discuss the results of parts (a)-(c) in terms of stability of the system.

Section B

The questions in this section are based on the paper reproduced at the end of this question paper. Devote at least half an hour to reading through the paper. Use your own words in your answers so as to demonstrate that you have understood the concepts described in the paper, do not copy extracts from the paper itself.

Q5. Explain the structure of a regular PID controller and a tuning method.

Q6. Discuss what the major problems in a MIMO control system.

Q7. Briefly explain the proposed tuning methodology in the paper.

Q8. What is the significance of the proposed methodology in tuning Fuzzy PID controller?

Design and Tuning of Standard Additive Model Based Fuzzy PID Controllers for Multivariable Process Systems

Eranda Harinath, *Student Member, IEEE*, and George K. I. Mann

***Abstract*—This paper describes a design and two-level tuning method for fuzzy proportional-integral derivative (FPID) controllers for a multivariable process where the fuzzy inference uses the inference of standard additive model. The proposed method can be used for any $n \times n$ multiinput–multioutput process and guarantees closed-loop stability. In the two-level tuning scheme, the tuning follows two steps: low-level tuning followed by high-level tuning. The low-level tuning adjusts apparent linear gains, whereas the high-level tuning changes the nonlinearity in the normalized fuzzy output. In this paper, two types of FPID configurations are considered, and their performances are evaluated by using a real-time multizone temperature control problem having a 3×3 process system.**

***Index Terms*—Fuzzy proportional-integral derivative (FPID) control, fuzzy standard additive model (SAM), linear PID tuning, multivariable control, multizone heating.**

I. Introduction

Among various techniques available in controlling multiinput–multioutput (MIMO) process systems, proportional-integral derivative (PID) controller loops are still popularly used in industry [1], [2]. Although PID design is simpler, tuning of its gains is always challenging for optimum operations. In the majority of MIMO applications [3]–[5], tuning is still performed by using the conventional single-input–single-output (SISO)-based Ziegler and Nichols (ZN) rules [6]. The design of controllers for an $n \times n$ MIMO system can be first considered as a task of designing n number of individual PID controllers. The individual loops can be tuned by using the SISO-based PID tuning rules. The decentralized control will become insufficient or sometimes will fail to provide better control in the presence of loop interactions. The loop interaction refers to the case where an input of a loop affects the other loops in the multivariable system. The detuning of ZN parameters sometimes helps to achieve a stable control. To address the effect of loop interactions, some researchers have attempted to use an interaction measure as an input to formulate PID parameter for MIMO processes [7]–[9]. Most of those applications are limited only for two-input two-output process systems. The complexity of the design method, in general, does not allow one to extend those methods for higher dimensional MIMO processes. Due to the PID controller's simplicity, the overall performance with respect to transient and steady-state operations is always poorer compared with other advanced techniques such as model predictive control systems. However, fuzzy PID (FPID) control has the ability to produce better response performances against linear PID systems. There is a huge volume of FPID applications available in the literature since the early work of Mamdani and Assilian [10]. The majority of applications belong to SISO process systems, and in a very few applications, MIMO systems have been considered [11]–[13]. In all these applications, the selection of FPID parameters is *ad hoc*, and the tuning is performed by using trial-and-error techniques.

The literature review revealed that there is no systematic design procedure that is available to design and tune FPID controllers for MIMO process systems. The available SISO-based FPID design techniques have limitations to extend for general MIMO systems with considerable interactions. Alternatively, this paper proposes a generalized tuning scheme for both linear PID and FPID controllers. The FPID controller follows the fuzzy inference based on the standard additive model (SAM), as proposed in [14]. The proposed tuning scheme follows two levels of tuning, namely, low-level tuning followed by high-level tuning [15].

This paper provides significant contributions in three aspects. First, a generalized FPID controller tuning mechanism using a two-level tuning principle is presented. The decomposition of linear and nonlinear tuning for FPID systems makes the design task of FPID systems simpler. Second, a novel linear PID gain tuning method is developed for MIMO process systems. Finally, high-performance SAM-based inference is employed to achieve superior control performance.

II. Two-Level Tuning

In a typical FPID design problem, the tuning parameters include linear scaling parameters of the control variables, fuzzy membership parameters, rules, and other associated fuzzy variables in the rule base, such as number of rules, membership distribution, and rule composition. The mathematical complexity in the nonlinear fuzzy control makes the formulation of a tuning mechanism an extremely complex problem. To ease

Manuscript received March 23, 2007; revised November 15, 2007. This work was supported by the Atlantic Innovation Fund. This paper was presented in part at the IEEE Conference on Decision and Control (CDC) 2007. This paper was recommended by Associate Editor M. de Queiroz.

E. Harinath is with the Department of Electrical and Computer Engineering, The University of British Columbia, Vancouver, BC V6T 1Z4, Canada (e-mail: eranda@ece.ubc.ca).

G. K. I. Mann is with the Faculty of Engineering and Applied Science, Memorial University of Newfoundland, St. John's, NF A1B 3X5, Canada.

Color versions of one or more of the figures in this paper are available online at http://ieeexplore.ieee.org.

Digital Object Identifier 10.1109/TSMCB.2008.919232

00041

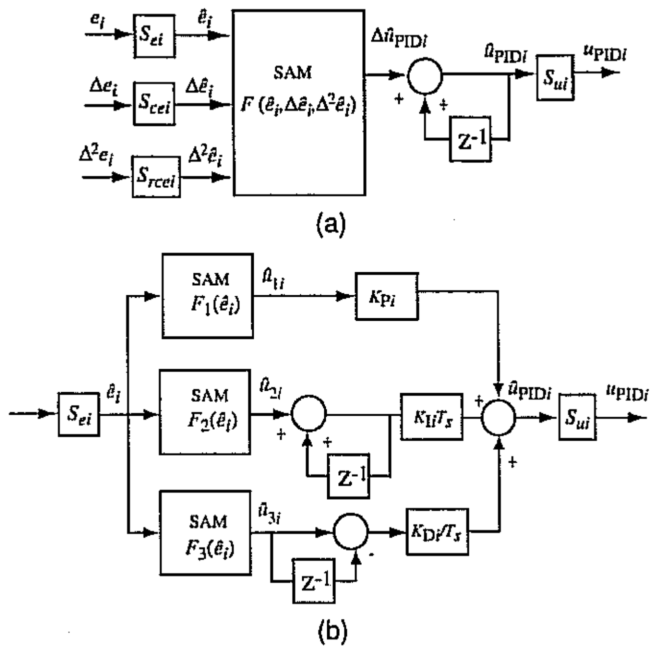

Fig. 1. FPID configurations. (a) Type I: Rule-coupled FPID. (b) Type II: Rule-decoupled FPID.

this complex tuning problem, the FPID design has been classified as a two-level tuning problem [15], in which the tuning process is decomposed into two tuning levels. While low-level tuning addresses the linear gain and overall stability, the high-level tuning provides nonlinear control to enable superior performance. In a Mamdani-based fuzzy-logic-controller (FLC) system, the inputs (error and its derivative) are coupled to produce a combined fuzzy PI output [15]. In order to facilitate the two-level tuning, we define apparent linear gains (ALGs) and apparent nonlinear gains (ANGs). While the ALG terms are related to the overall performance and stability of the system, the ANG terms provide the nonlinearity that is necessary in the fuzzy output.

III. FPID Configurations

Two types of FPID configurations are considered, as shown in Fig. 1. The type I shown in the figure is a conventional Mamdani-type FPID, which produces an incremental coupled FPID signal. The type II uses SISO rule inference to provide decoupled three actions in the PID signal. By using suitable scale factors (S_{wi}), where $w = 1, 2, 3$, the feedback error terms (e_i) and its corresponding normalized error variables ($\hat{e}_i$) at kth sampling instance can be expressed as: $\hat{e}_i(k) = S_{1i}\ e_i(k)$, $\Delta\hat{e}_i(k) = S_{2i}\Delta e_i(k)$, and $\Delta^2\hat{e}_i(k) = S_{3i}\Delta^2 e_i(k)$. All FLC input variables are normalized to a compact region $[-1, 1]$. The error variables are normalized by using the condition $\hat{e}_{wi} = \max(-1, \min(1, S_{wi}e_{wi}))$. The defuzzified controller output after the fuzzy inference is denoted by $\hat{u}$. Similarly, the FLC output is normalized by using the condition $\hat{u} \equiv u/u_{\max}$.

A. High-Level Nonlinear Tuning Variables

The nonlinear tuning variables are selected to affect the ANG terms at any given local control point in the control surface. Since PID gains are proportional to the slopes of the control surface, the slope angles of the tangents drawn at a given point on the nonlinear control surface are considered to be the nonlinear tuning variables. Two slope angles drawn at two selected points, i.e., $\hat{e} = 0$ and $\hat{e} = 1$ (see Fig. 2), on the control surface are considered as the nonlinear tuning variables.

In order to isolate slope angles from their associated outputs of FPID type I controller, the slopes are measured in the planes of individual error axes. The measurement of these angles with respect to a 2-D control surface is shown in Fig. 2(a). Fig. 2(b) shows a control curve that has been projected into a chosen error variable. In general, for a three-input coupled rule base, the slope angles can be described as: $(\theta_0)_{wi} = (\partial\hat{u}_f/\partial\hat{e}_{wi})_{\hat{e}_{wi}=-1}$ and $(\theta_1)_{wi} = (\partial\hat{u}_f/\partial\hat{e}_{wi})_{\hat{e}_{wi}=1}$, where $\hat{u}_f = \hat{u}(\hat{e}_p = 0)$, $p = 1, 2, 3$, $p \neq w$. The fuzzy system designed for the PID control should allow independent variations of θ_0 and θ_1 within the range $[0\ 90°]$.

B. Low-Level Linear Tuning Variables

The composed FPID control action for FPID type I is given by

$$u_{\mathrm{PID}i} = S_{ui}\sum_{r=0}^{k}\Delta\hat{u}_{\mathrm{PID}i}(r). \tag{1}$$

Referring to Fig. 1(b), the FPID action for FPID type II can be expressed as

$$u_{\mathrm{PID}i} = S_{ui}\left[K_{\mathrm{P}i}\hat{u}_{1i} + K_{\mathrm{I}i}T_s\sum_{r=0}^{k}\hat{u}_{2i}(r) + \frac{K_{\mathrm{D}i}}{T_s}\left(\hat{u}_{3i}(k) - \hat{u}_{3i}(k-1)\right)\right] \tag{2}$$

where $K_{\mathrm{P}i}$, $K_{\mathrm{I}i}$, and $K_{\mathrm{D}i}$ are the linear PID gains for the ith loop, and T_s is the sampling time. When a fuzzy system is set to produce a linear function, the FLC will become a linear-type PID controller and is defined as an equivalent linear controller (ELC). By using the ELC output, the ith loop linear PID output can be arranged in the following form:

$$u^l_{\mathrm{PID}i}(k) = K_{\mathrm{Pa}i}e_i(k) + K_{\mathrm{Ia}i}\sum_{r=0}^{k}e_i(r)T_s + K_{\mathrm{Da}i}\Delta e_i(k)/T_s \tag{3}$$

where $K_{\mathrm{Pa}i}$, $K_{\mathrm{Ia}i}$, and $K_{\mathrm{Da}i}$ are defined as the ALG terms of the FLC system. An FLC having a linear rule base and a uniform partition of universe of discourse of all variables is named as a linearlike FLC (LLFLC). The ELC defined for the LLFLC is used to derive the linear tuning variables. Then, the ELC output for type I is given by

$$\Delta\hat{u}^l_{\mathrm{PID}i} = [\hat{e}_i + \Delta\hat{e}_i + \Delta^2\hat{e}_i]. \tag{4}$$

From (3) and (4), the ALG terms can be found as

$$K_{\mathrm{Pa}i} = S_u S_{2i} \quad K_{\mathrm{Ia}i} = S_u S_{1i}/T_s \quad K_{\mathrm{Da}i} = S_u S_{3i}T_s. \tag{5}$$

00041

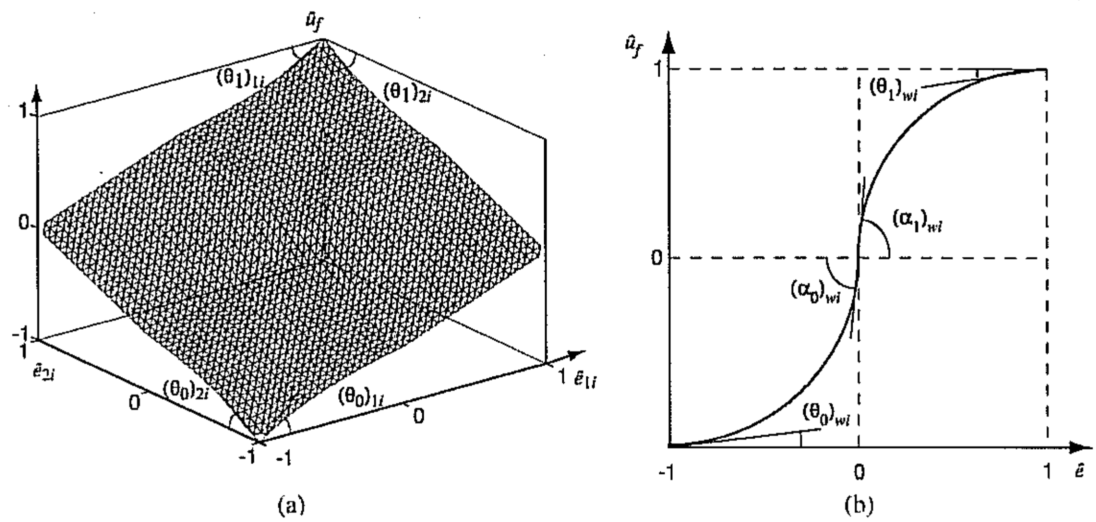

Fig. 2. Nonlinear tuning variables measured at local control points for FPID configurations.

Similarly, the ELC output for type II is given by $\hat{u}^l_{1i} = \hat{u}^l_{2i} = \hat{u}^l_{3i} = \hat{e}_i$. Thus, the ALG terms can be found as

$$K_{\mathrm{Pa}i} = K_{pi} \quad K_{\mathrm{Ia}i} = K_{\mathrm{I}i} \quad K_{\mathrm{Da}i} = K_{\mathrm{D}i}. \tag{6}$$

The adjustment of K_{Pa}, K_{Da}, and K_{Ia} refers to a general PID tuning with the control surface normalized to a linear form in the normalized output space. The ANG terms refer to the effect of changing the nonlinearity of the FPID output in the nonlinearity output space.

IV. Low-Level Tuning: Linear PID Controller Tuning

The n-input n-output process with a static decoupler and an FPID controller is shown in Fig. 3 where the multivariable system is assumed as a linear and open-loop stable system. The proposed tuning mechanism allows one to use linear tuning methodologies in order to obtain linear FPID parameters in a form of ALG values. The main challenge of interactions among loops has been minimized by using a static decoupler. For a general $n \times n$ MIMO process, similar analysis is described in [16]. For this paper, only the final expressions required for ALG tuning are presented. The decentralized PID parameter for the ith loop can be then expressed as [16]

$$K_{\mathrm{I}i} = \frac{I_i}{\max_{i \neq j}\left(|K_{ij}|\right)(S_i)_{\max}} \tag{7}$$

$$K_{\mathrm{P}i} = \frac{1 \pm \zeta_i \sqrt{K_{\mathrm{I}i}^2 - 4\zeta_i^2 K_{\mathrm{I}i}^3 T_{ii} + 4K_{\mathrm{I}i} T_{ii}^2}}{4K_{\mathrm{I}i}^2 \zeta_i^2 - 1} \tag{8}$$

$$K_{\mathrm{D}i} = \frac{K_{\mathrm{P}i}^2}{4K_{\mathrm{I}i}} \tag{9}$$

where I_i is the interaction index, S_i is the loop sensitivity function, K_{ij} is the off-diagonal parameter, T_{ii} is the time constant, and ζ_i is the damping constant. In this design, we use the aforementioned tuning parameters for low-level tuning.

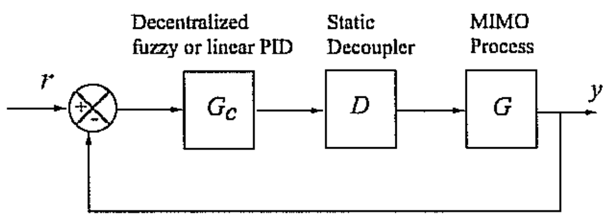

Fig. 3. Statically decoupled multivariable control.

V. High-Level Tuning: Nonlinearity Tuning

The high-level tuning is dedicated to determine fuzzy rule-base parameters, which has a direct relevance to the nonlinearity of the FLC output. The nonlinearity that is generated through fuzzy mapping is then adjusted by using high-level tuning parameters. In general, the nonlinearity can be adjusted either by changing rules or by changing knowledge base rule parameters, such as membership shapes and their distributions in the universe of discourse of variables. An effective nonlinearity tuning mechanism should have the capacity to produce a flexibility to change the nonlinearity of the fuzzy output in a wider range. A proper selection of a fuzzy inference mechanism is quite important in achieving an efficient high-level tuning [17]. It is found that SAM-based fuzzy inference has the capacity to provide better nonlinearity tuning as opposed to traditional min–max-gravity inference [16]. SAM is a special case of the additive model framework shown in Fig. 4, and the following can be observed as special properties in SAM.

1) The fired then-part set B'_β is the fit product $a_\beta(x)B_\beta$, where the fit value $a_\beta(x)$ (a_β is called membership function) expresses the membership grade of input x in the if-part fuzzy set A_α. Then, the output set can be expressed as

$$B = \sum_{\beta=1}^{m} w_\beta a_\beta(x) B_\beta(x). \tag{10}$$

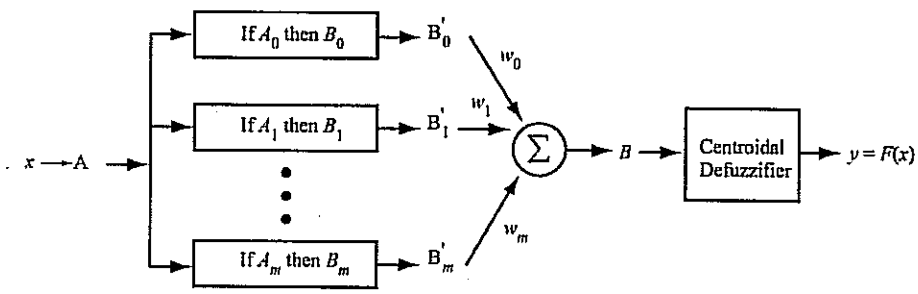

Fig. 4. General framework of additive fuzzy system.

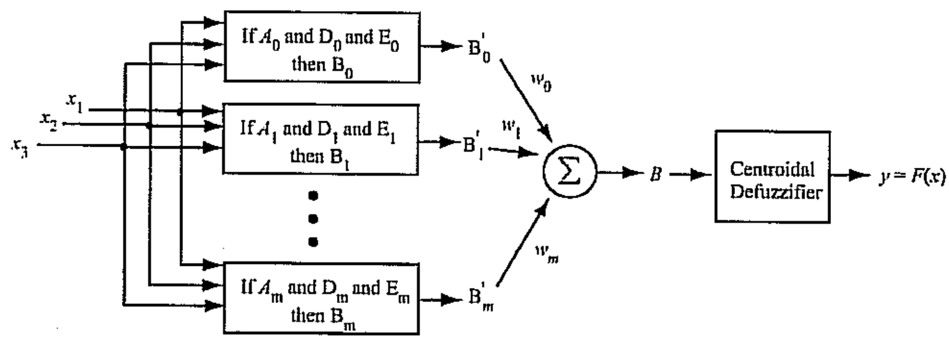

Fig. 5. SAM representation of rule-coupled fuzzy system.

2) The system output $F(x)$ computes as centroid of output set $B(x)$ and defuzzifies to a scalar or a vector

$$F(x) = \text{Centroid}\left(\sum_{\beta=1}^{m} w_\beta a_\beta(x) B_\beta(x)\right). \quad (11)$$

The centroid provides the structure of a conditional expectation to the fuzzy system F, and it acts as an optimal nonlinear approximator in the mean-squared sense.

VI. Design of SAM for FPID Configurations

A. Rule Coupled

Fig. 5 shows the SAM representation of rule coupled (FPID type I) for three-input–single-output system. In this design, we have selected membership functions (a_i) for the if-part in SAM as triangle functions, as shown in the Fig. 6. With the min combiner, the SAM output for the aforementioned system can be written as

$$F(x) = \frac{\sum_{\beta=1}^{m} w_\beta \min\{a_\beta(x_1), a_\beta(x_2), a_\beta(x_3)\}\, V_\beta C_\beta}{\sum_{\beta=1}^{m} w_\beta \min\{a_\beta(x_1), a_\beta(x_2), a_\beta(x_3)\}\, V_\beta}. \quad (12)$$

Since each rule uses one (min of fired membership values) of the three inputs to defuzzy, it is equivalent to a SISO SAM system. In other words, the analysis of rule-coupled FPID configuration in the view of SAM is similar to the rule-decoupled FPID configuration.

B. Rule Decoupled

Consider two control regions in the controller output space. The first region is when the normalized error variables are $-1 \le \hat{e}_i < 0$. The local control in this region affects steady state, load disturbance, and overshoot properties. The second region is when $0 \le \hat{e}_i \le 1$. The control in this region affects the speed of response during the transient, undershoot, and steady-state properties. The objective is to realize independent adjustment of FLC parameters in the view of changing ANG terms at the chosen control points. The slope angle θ for type II [see Fig. 2(b)] can be described as follows.

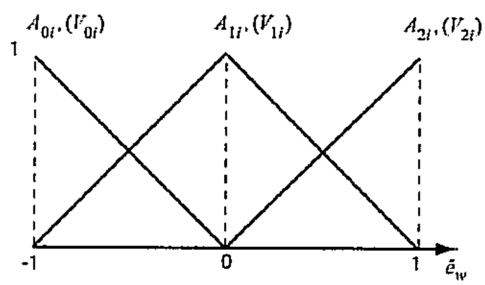

Fig. 6. Membership functions for the if-part in SAM.

Consider the ith loop fuzzy controller (for example, P controller) in Fig. 2(b), and it is shown in Fig. 7. The membership function for the if-part in this controller is described by using Fig. 6. From (11), SAM output $\hat{u}_{1i}$ can be described by

$$\hat{u}_{1i} = \frac{-\hat{e}_i V_{0i} C_{0i} + (\hat{e}_i + 1) V_{1i} C_{1i}}{-\hat{e}_i V_{0i} + (\hat{e}_i + 1) V_{1i}}, \quad \text{for } -1 \le \hat{e}_i < 0$$

$$\hat{u}_{1i} = \frac{\hat{e}_i V_{2i} C_{2i} - (\hat{e}_i - 1) V_{1i} C_{1i}}{\hat{e}_i V_{2i} - (\hat{e}_i - 1) V_{1i}}, \quad \text{for } 0 \le \hat{e}_i \le 1.$$

Then, the slope of $\hat{u}_{1i}$ with respect to $\hat{e}_i$ is

$$\tan\theta = \frac{d\hat{u}_{1i}}{d\hat{e}_i}.$$

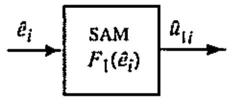

Fig. 7. High-level fuzzy controller.

Thus, θ is expressed as (13), shown at the bottom of the page. In this analysis, the then-part centroid C_{wi} is selected as

$$C_{0i} = -1 \quad C_{1i} = 0 \quad C_{2i} = 1. \tag{14}$$

The stability properties are determined by the extreme values of equivalent PID gains. Therefore, to guarantee stability, the maximum and minimum ANG terms are considered in an equivalent linear PID system. In the SAM inference, the maximum or minimum of ANG occurs when $\hat{e}_i = -1$, $\hat{e}_i = 0$, and $\hat{e}_i = 1$. Then, the slope angles at selected four points (see Fig. 2) are as follows:

$$(\theta_0)_{wi} = \arctan(V_{1i}/V_{0i}) \quad (\alpha_0)_{wi} = \arctan(V_{0i}/V_{1i}) \tag{15}$$

$$(\theta_1)_{wi} = \arctan(V_{1i}/V_{2i}) \quad (\alpha_1)_{wi} = \arctan(V_{2i}/V_{1i}). \tag{16}$$

It is clear that the pairs $\{(\theta_0)_{wi}, (\alpha_0)_{wi}\}$ and $\{(\theta_1)_{wi}, (\alpha_1)_{wi}\}$ form a right angle. There are two independent slope angles that can be defined over the control surface of SAM corresponding to two regions $-1 \le \hat{e}_i < 0$ and $0 \le \hat{e}_i \le 1$. Therefore, we select $(\theta_0)_{wi}$ and $(\theta_1)_{wi}$ as the two independent slope angles to be adjusted within the range of [0 90°] for high-level tuning. In order to find two independent angles, the then-part volume for second membership function is selected as unity: $V_{1i} = 1$. Then

$$\theta_0 = \arctan(1/V_0) \quad \theta_1 = \arctan(1/V_2). \tag{17}$$

Hence, the terms V_0 and V_2 are the nonlinear tuning variables for the SAM.

VII. Stability Analysis

Ho Weng *et al.* [18] have given the definitions for the gain and phase margins of MIMO systems using a Nyquist diagram. In order to guarantee stability, according to the DNA stability theorem [19], the Gershgorin bands should be shaped based on predefined values of phase margin (ϕ_i') and gain margin (α_i') so that it excludes and does not encircle the point $(-1 + \jmath 0)$. As a rule of thumb, ϕ_i' and α_i' should satisfy the following conditions:

$$30° \le \phi_i' \le 60° \qquad 2 \le \alpha_i' \le 5.$$

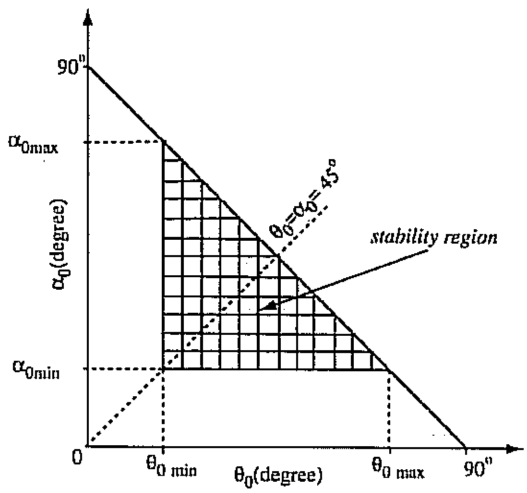

Fig. 8. Stability region for θ_0 and α_0. It is the same for θ_1 and α_1.

Then, the hard limits of PI parameters can be calculated as in [18] so that we can define

$$K_{Pi\,max} \qquad K_{Ii\,max} \tag{18}$$

as maximum values of PI parameters at a given ϕ_i' and α_i'. From (9)

$$K_{Di\,max} = \frac{K_{Pi\,max}^2}{4K_{Ii\,max}}. \tag{19}$$

Since PID gains are proportional to the slopes of the control surface shown in Fig. 2, we can find maximum values of slope angle corresponding to $K_{Pi\,max}$, $K_{Ii\,max}$, and $K_{Di\,max}$. For instance, let the proportional SAM-based fuzzy controller for ith be with high-level tuning parameters: V_0 and V_2. From (15) and (16), the following expression can be derived:

$$\begin{aligned} V_{0\,min} &= V_{2\,min} = K_{Pi}/K_{Pi\,max} \\ V_{0\,max} &= V_{2\,max} = K_{Pi\,max}/K_{Pi}. \end{aligned} \tag{20}$$

Then, limiting angles for θ_0, α_0, θ_1, and α_1 can be expressed as

$$\begin{aligned} \theta_{0\,max}, \alpha_{0\,max}, \theta_{1\,max}, \alpha_{1\,max} &= \arctan(K_{Pi\,max}/K_{Pi}) \\ \theta_{0\,min}, \alpha_{0\,min}, \theta_{1\,min}, \alpha_{1\,min} &= \arctan(K_{Pi}/K_{Pi\,max}). \end{aligned} \tag{21}$$

If $\{K_{Pi\,max}/K_{Pi} \ge 1.571\}$, the fuzzy controller has independent variations of θ_0 and θ_1 within the range [0 90°]. Otherwise, it has a feasible stability region, as shown in Fig. 8.

VIII. Real-Time Experiments

The objective of experiments is to control temperatures at three different locations of soil cell by using three different heaters. The schematic diagram of the experimental setup is

---

$$\theta = \begin{cases} \arctan\left(\frac{V_{0i}(2\hat{e}_i V_{0i} C_{0i} - 2C_{0i} V_{1i} \hat{e}_i - C_{0i} V_{1i} + V_{1i} C_{1i})}{(\hat{e}_i V_{0i} - \hat{e}_i V_{1i} - V_{1i})^2}\right), & \text{for } -1 \le \hat{e}_i < 0 \\ \arctan\left(-\frac{V_{2i} V_{1i}(-C_{2i} + C_{1i})}{(V_{1i}\hat{e}_i - V_{1i} - V_{2i}\hat{e}_i)^2}\right), & \text{for } 0 \le \hat{e}_i \le 1 \end{cases} \tag{13}$$

00041

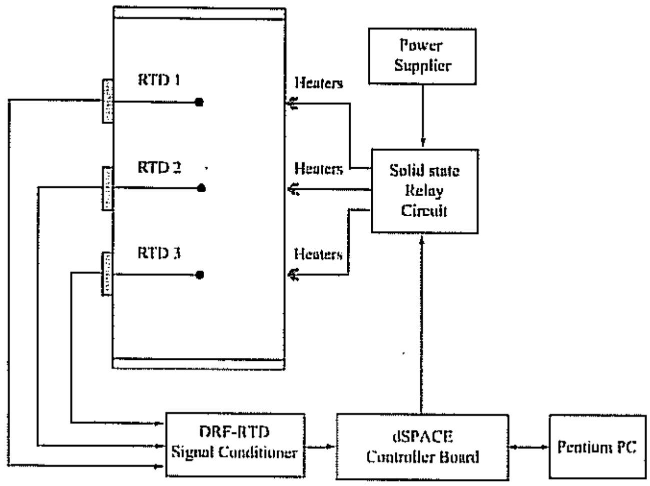

Fig. 9. Schematic of the multizone heating soil-cell experimental system.

shown in Fig. 9. The system identification is performed for a soil cell via the classical step response method. The transfer-function matrix $G(s)$ is developed by using the plant reaction curve method [20]. The control objective is to maintain different desired temperatures in three different locations. The control interface and the signal processing are implemented by using the dSPACE (DS1103) control prototype. The power at each heater (0–14 W) is manipulated while changing the duty cycle through solid-state relays. RTD temperature sensors have been used for temperature measurements and sampled at 1 Hz. The multizone heating problem provides a unique application where interactions between loops are considerable, and therefore, design of a stable controller is a challenging task. Due to the very low thermal conductivity of dry soil, the experiments were carried out for several hours (8000 min). Therefore, the effect of changing room temperatures provides additional disturbances to the system.

A. Open-Loop Test

In the open-loop test, a total of nine response curves has been used to estimate the overall transfer function, where each test constitutes a corresponding open-loop response corresponding to a given input. The temperature responses with respect to room temperatures are modeled, and the final transfer function is given next. It should be noted that the effect of the first heater on the temperature at the lowest point is quite minimal and approximately $G_{31} = G_{13} \approx 0$

$$G(s) = \begin{bmatrix} \frac{13.42e^{-54s}}{168s+1} & \frac{5e^{-487s}}{397.5s+1} & 0 \\ \frac{3.019e^{-184s}}{258s+1} & \frac{19.8e^{-99s}}{462s+1} & \frac{4.1e^{-271s}}{313.5s+1} \\ 0 & \frac{2.25e^{-553s}}{358.5s+1} & \frac{12.5e^{-55.5s}}{178.5s+1} \end{bmatrix}. \quad (22)$$

B. Implementation of Control Algorithms

Three different types of control algorithms, namely, PID, FPID type I, and FPID type II, are implemented to control temperatures. The average room temperature during the experiments was 22 °C. In these control experiments, the set-point

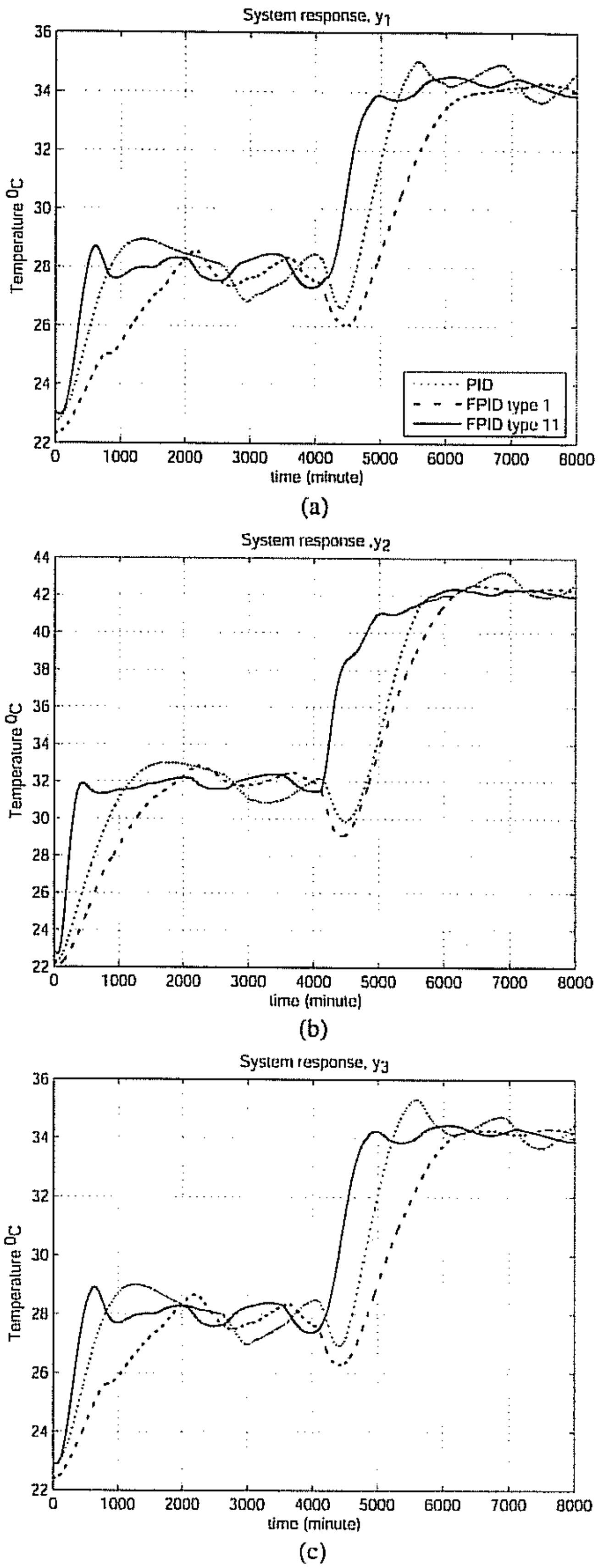

Fig. 10. Real-time experiments. Closed-loop tests of soil cell. (a) Output1. (b) Output2. (c) Output3.

TABLE I
PERFORMANCE CHARACTERISTIC INDEXES OF THE PROPOSED FPID METHODS AND PID METHOD FOR SET-POINT TRACKING

Output	Set Point Tracking								
	Rise Time/minute			Overshoot %			Setting Time/minute		
	PID	FPID1	FPID2	PID	FPID1	FPID2	PID	FPID1	FPID2
y_1	740	1700	445	16.7	10.0	11.7	2300	3670	1000
y_2	730	1080	260	10.0	9.0	3.0	3750	2500	960
y_3	700	1590	425	17.7	11.7	15.8	2050	3550	1000

TABLE II
SET POINT TEMPERATURES ASSIGNED FOR EACH OUTPUT IN THE CONTROL EXPERIMENTS FOR THE OPEN-LOOP TEST

Time t (min)	Output 1	Output 2	Output 3
$0 \leq t < 4000$	28 °C	32 °C	28 °C
$4000 \leq t < 8000$	34 °C	42 °C	34 °C

TABLE III
GAIN AND PHASE MARGINS OF EACH LOOP OF THE SOIL CELL

loop No	Gain Margin	Phase Margin
1	2.4	40°
2	3.6	35°
3	5.5	45°

temperatures assigned for each output are shown in Table II. It is important to note that the highest set-point temperature is assigned for the middle zone, which makes the interactions to other two zones significant. Fig. 10 shows the responses of each system. In this design, first, the linear PID values have been chosen by using the new PID law, and then, the nonlinear parameters (V_1 and V_2) were tuned to obtain a better performance. The FPID-I system constitutes a coupled rule base, and the fuzzy inference requires both first and second derivatives of the error. This particular characteristic is termed as the input composition [21]. As a result, the FPID type I responses are slower. Due to the coupled nature, the nonlinearity change that can be accommodated for each action is somewhat limited. It is possible to change the overall gain, but this will cause the interactions to be higher and makes tuning a more difficult problem. In PID control system, speed of response is moderate but has shown higher overshoot and longer settling time. The nonlinear tuning in FPID-II is able to produce a better performance. This is mainly due to the change of overall gain values at the set points. The nonlinear tuning allows one to adjust the PID gains locally by changing the slope angles. The speed of response has been improved due to the increased overall gain values at the beginning of the response. This is the key advantage in FPID tuning, where the speed of response can be improved while changing the slope angles. The independent adjustment of slope angles allows one to alter the speed of response without affecting the steady-state behavior. The temperature variations in the steady-state values of the systems are due to the fluctuations of the room temperature. It can be seen that all the systems show an inverse response due to the nonminimum phase characteristic of the soil cell. The performance characteristics derived from all the experiments are shown in Table I. The gain and phase margins for individual loop are shown in Table III. The results reveal that the gain and phase margins derived for all the experiments are within the specified limits, as proposed in [18]. Therefore, the very loop confirms to the DNA stability theorem.

The following steps summarize the systematic design procedure.

1) Equivalent first-order delayed models are found for all higher order subprocesses by analyzing the response using plant reaction curve methods.
2) The static decoupler is obtained for MIMO process.
3) An equivalent first-order model for the overall compensated system (first-order model with static decoupler) is obtained by using truncated Taylor series approximation at low frequencies.
4) A measure of interaction is developed, and integral gains are calculated for each loop at particular values of interaction indexes.
5) By using direct pole placement method [22] and ZN [6] tuning formulas, proportional and derivative gains of linear PID controllers are calculated for low-level tuning.
6) SAM is developed for MIMO process, and high-level tuning parameters are identified in order to have an optimum nonlinearity in the fuzzy output.
7) Different types of FPID configurations are considered for the design of SAM.
8) Nonlinear tuning parameters (volumes of the then-part fuzzy in SAM) are tuned for each FPID configuration so that the overall system is stable.

IX. CONCLUSION

Design and tuning of decoupled SAM-based FPID controllers for a general $n \times n$ MIMO process system has been presented. The design of an FPID is treated as a two-level tuning problem. In this proposed fuzzy tuning, the linear PID can become a special class of the FPID when the nonlinearity is adjusted to provide a linear output surface or LLFLC [21]. It is quite important to note that the most popular Mamdani-type FPID (FPID type 1) has shown the worst performance and is unable to perform any better than the linear PID system. The loop interaction is generally minimized with lesser integral action. As compared with the SISO PID system, the loop interaction does not allow the increase of the PID parameter without compromising other gains in the system. The input coupling that exists in the Mamdani-type FPID systems does not have the capacity to change the PID actions or the integral gains independently. Therefore, any alterations to the steady-state values have an effect on the transient. Thus, we can conclude that the Mamdani-type FPID systems have some limitations when used in multivariable control systems. However, when the rules are decoupled (FPID-type II), the fuzzy controller has the ability to outperform the linear PID system. The performance of controllers has been compared for the 3 × 3 MIMO multizone heating process systems. The interactions that exist between loops make this application a better test platform to design multivariable controllers.

ACKNOWLEDGMENT

The authors would like to thank the Memorial University for the graduate support. This paper is undertaken as part of the Pan-Atlantic Petroleum System Consortium Project at the Memorial University of Newfoundland.

REFERENCES

[1] J. Dong and C. B. Brosilow, "Design of robust multivariable PID controllers via IMC," in *Proc. Amer. Control Conf.*, Jun. 4–6, 1997, vol. 5, pp. 3380–3384.
[2] S. Yamamoto and I. Hashimoto, "Present status and future needs: The view of from Japanese industry," in *Proc. 4th Int. Conf. Chem. Process Control*, I. Arkun and I. Ray, Eds., 1991, pp. 1–28.
[3] A. Niederlinski, "A heuristic approach to the design of linear multivariable interacting control systems," *Automatica*, vol. 7, pp. 691–701, 1971.
[4] W. L. Luyben, "Simple method for tuning SISO controllers in multivariable systems," *Ind. Eng. Chem. Process Des. Dev.*, vol. 25, no. 3, pp. 654–660, Jul. 1986.
[5] D. Chen and D. E. Seborg, "Multiloop PI/PID controller design based on gershgorin bands," in *Proc. Amer. Control Conf.*, Jun. 25–27, 2001, vol. 5, pp. 4122–4127.
[6] J. G. Ziegler and N. B. Nichols, "Optimum settings for automatic controllers," *Trans. ASME*, vol. 64, pp. 759–768, 1942.
[7] M. Witcher and T. J. McAvoy, "Interacting control systems: Steady state and dynamic measurement of interaction," *ISA Trans.*, vol. 16, no. 3, pp. 35–41, 1977.
[8] K. J. Astrom, K. H. Johansson, and Q.-G. Wang, "Design of decoupled PID controllers for MIMO systems," in *Proc. Amer. Control Conf.*, Jun. 2001, vol. 3, pp. 2015–2020.
[9] J. Lee and T. F. Edgar, "Interaction measure for decentralized control of multivariable processes," in *Proc. Amer. Control Conf.*, May 2002, vol. 1, pp. 454–458.
[10] E. H. Mamdani and S. Assilan, "An experiment in linguistic synthesis with a fuzzy logic controller," *Int. J. Man-Mach. Stud.*, vol. 7, no. 1, pp. 1–13, 1975.
[11] G. I. Eduardo and M. R. Hiram, "Fuzzy multivariable control of a class of a biotechnology process," in *Proc. IEEE Int. Symp. Ind. Electron.*, Jul. 1999, vol. 1, pp. 419–424.
[12] A. Rahmati, F. Rashidi, and M. Rashidi, "A hybrid fuzzy logic and PID controller for control of nonlinear HVAC systems," in *Proc. IEEE Int. Conf. Syst., Man and Cybern.*, Oct. 2003, vol. 3, pp. 2249–2254.
[13] S. Li, H. Liu, W.-J. Cai, Y.-C. Soh, and L.-H. Xie, "A new coordinated control strategy for boiler-turbine system of coal-fired power plant," *IEEE Trans. Control Syst. Technol.*, vol. 13, no. 6, pp. 943–954, Nov. 2005.
[14] B. Kosko, *Fuzzy Engineering*. Upper Saddle River, NJ: Prentice-Hall, 1997.
[15] G. K. I. Mann, B.-G. Hu, and R. G. Gosine, "Two-level tuning of fuzzy PID controllers," *IEEE Trans. Syst., Man Cybern. B, Cybern.*, vol. 31, no. 2, pp. 263–269, Apr. 2001.
[16] E. Harinath, "Design and tuning of fuzzy PID controllers for multivariable process systems," M.S. thesis, Memorial Univ. Newfoundland, St. John's, NL, Canada, 2007.
[17] B. Hu, G. K. I. Mann, and R. G. Gosine, "New methodology for analytical and optimal design of fuzzy PID controllers," *IEEE Trans. Fuzzy Syst.*, vol. 7, no. 5, pp. 521–539, Oct. 1999.
[18] K. Ho Weng, H. Lee Tong, and O. P. Gan, "Tuning of multiloop proportional-intergral-derivative controllers based on gain and phase margin specifications," *Ind. Eng. Chem. Res.*, vol. 36, pp. 2231–2238, 1997.
[19] H. H. Rosenbrock, *State-Space and Multivariable Theory*. London, U.K.: Nelson, 1970.
[20] E. F. Camacho and C. Bordons, *Model Predictive Control*. London, U.K.: Springer-Verlag, 1999.
[21] G. K. I. Mann, B.-G. Hu, and R. G. Gosine, "Analysis of direct action fuzzy PID controller structures," *IEEE Trans. Syst., Man Cybern. B, Cybern.*, vol. 29, no. 3, pp. 371–388, Jun. 1999.
[22] K. J. Astrom and T. Hagglund, *PID Controllers: Theory, Design and Tuning*. Research Triangle Park, NC: Instrum. Soc. Amer., 1995.

Eranda Harinath (S'06) received the B.Sc. degree in electrical engineering from the University of Moratuwa, Moratuwa, Sri Lanka, in 2003, and the M.Eng. degree in electrical and computer engineering from the Memorial University of Newfoundland, St. John's, NF, Canada, in 2007. He is currently working toward the Ph.D. degree in the Department of Electrical and Computer Engineering, The University of British Columbia, Vancouver, BC, Canada.

His current research interests include intelligent control of multivariable process and application of model predictive control in pulp and paper industries.

George K. I. Mann received the B.Sc. (Hons.) engineering degree from the University of Moratuwa, Moratuwa, Sri Lanka, the M.Sc. degree in computer-integrated manufacture from Loughborough University, Leicestershire, U.K., and the Ph.D. degree from the Memorial University of Newfoundland, St. John's, NF, Canada, in 1999.

After completing his doctoral studies, he was with C-CORE, Memorial University of Newfoundland, for two years as a Research Engineer. In 2001, he was with the Mechanical Engineering Department, Queen's University, Kingston, ON, Canada, as a Postdoctoral Fellow while supported by an NSERC postdoctoral fellowship. Before he came to Canada, he was a Lecturer with the Department of Mechanical Engineering, University of Moratuwa. He is currently an Associate Professor with the Faculty of Engineering and Applied Science, Memorial University of Newfoundland. He also holds the C-CORE Junior Chair position in Intelligent Systems at Memorial University. His main research areas are intelligent control, robotics, and machine vision.